RSC Advances

PAPER

View Article Online
View Journal | View Issue

Cite this: *RSC Adv.*, 2016, **6**, 29314

The saturation of the gas phase acidity of nHF/AlF_3 and nHF/GeF_4 (n = 1–6) superacids caused by increasing the number of surrounding HF molecules†

Marcin Czapla,[a] Iwona Anusiewicz[ab] and Piotr Skurski*[ab]

Received 25th January 2016
Accepted 14th March 2016

DOI: 10.1039/c6ra02199a

www.rsc.org/advances

The acidic strength of selected Brønsted/Lewis superacids is evaluated on the basis of theoretical calculations carried out at the QCISD/6-311++G(d,p) level. The energies and Gibbs free energies of deprotonation processes for nHF/AlF_3 and nHF/GeF_4 (n = 1–6) are found to depend on the number (n) of hydrogen fluoride molecules (playing a Brønsted acid role) surrounding the AlF_3 and GeF_4 Lewis acids. The successive attachment of HF molecules to either AlF_3 or GeF_4 gradually increases the acidity strength of the resulting superacid, which leads to the saturation achieved for 5–6 HF molecules interacting with either one of these Lewis acids. The importance of the microsolvation of the corresponding anionic species as well as the necessity of considering larger (more structurally complex) building blocks of superacids while predicting their acidity is indicated and discussed.

1. Introduction

Superacids are commonly considered as compounds exhibiting acidity stronger than 100% sulfuric acid, which means that their Hammett acidity function (H_0) is smaller than −12.[1,2] Even though this term was used for the very first time in 1927,[3] the superacid chemistry was developed mainly in the 1960s and 1970s by Olah and Hogeveen, who investigated non-aqueous HSO_3F/SbF_5 and HF/SbF_5 systems,[4–9] and by Gillespie.[1,2] Since then, superacids remain the subject of continuing theoretical[10–13] and experimental[14–19] investigations concerning their structure, stability and acidity. Our group contributed to these studies by addressing the issue of the $HAlCl_4$ instability,[20] predicting the acidic strength of the aluminum-based HF/AlF_3 ($HAlF_4$), HF/Al_2F_6 (HAl_2F_7), HF/Al_3F_9 (HAl_3F_{10}), and HF/Al_4F_{12} (HAl_4F_{13}) systems,[21] investigating the dissociative excess electron attachment to the $HAlF_4$ superacid[22] (whose properties were earlier determined by the Radom group[23,24]), examining the strength of the Brønsted/Lewis superacids containing In, Sn, and Sb (*i.e.*, HIn_nF_{3n+1}, HSn_nF_{4n+1}, and HSb_nF_{5n+1} (n = 1–3)),[25] and, most recently, by demonstrating that the protonation of superhalogen anions[26,27] might be considered as the route to superacids' formation in selected cases only,[28] despite the fact that various superhalogens containing heavy metals as central atoms (*e.g.*, InF_4, SbF_6, Sb_2F_{11}, SnF_5, Sn_2F_9) were utilized in the past to create atypical salts and complexes[29–35] even with noble gases (Kr and Xe).[36–39]

The Lewis–Brønsted superacids consist of strong Lewis acid molecules (such as AlF_3) interacting with strong Brønsted acid molecules (*e.g.*, HF) and thus their deprotonation process might be described by the following reaction scheme (that assumes the excess of a representative Brønsted acid):

$$n\mathrm{HF/AlF_3} \rightarrow ((n-1)\mathrm{HF/AlF_4})^- + \mathrm{H}^+.$$

Clearly, the microsolvation of an anionic species (whose role is played by the AlF_4^- in the above scheme) is expected to be responsible for the change in energy with respect to the neutral microsolvated species. The Gibbs free energies of the superacid deprotonation reactions (ΔG_{acid}) are commonly utilized while describing the acidity of superacids. Although estimated only for the gas phase, the ΔG_{acid} values were found useful in designing novel systems exhibiting significant acidity. It is worth noting that the strongest superacids proposed thus far were found to possess their Gibbs free energies of deprotonation in the 249–270 kcal mol^{-1} range.[11] Most recently, Srivastava and Misra also reported small ΔG_{acid} values (indicating strong acidity) for $HBeCl_3$ (272 kcal mol^{-1}), HPF_6 (281 kcal mol^{-1}), and $HLiCl_2$ (284 kcal mol^{-1}),[13] whereas our group demonstrated that even smaller Gibbs free deprotonation energies are estimated for $HGaCl_4$ (265 kcal mol^{-1}),[28] HSn_3F_{13} (244 kcal mol^{-1}),[25] HAl_4F_{13} (249 kcal mol^{-1}),[21] and HSb_3F_{16} (230 kcal mol^{-1}).[25] In fact, the last

[a]*Laboratory of Quantum Chemistry, Faculty of Chemistry, University of Gdańsk, Wita Stwosza 63, 80-308 Gdańsk, Poland. E-mail: piotr.skurski@ug.edu.pl*

[b]*Department of Technical Physics and Applied Mathematics, Gdańsk University of Technology, Narutowicza 11/12, 80-233 Gdańsk, Poland*

† Electronic supplementary information (ESI) available: The Cartesian coordinates of all the structures presented in this work and their corresponding energies are included. See DOI: 10.1039/c6ra02199a

presented ΔG_{acid} value of 230 kcal mol^{-1} predicted for the HF/Sb_3F_{15} represents[25] the smallest gas phase Gibbs free energy of deprotonation reported in the literature thus far (including the corresponding values characterizing $F(SO_3)_4H$ and $HSbF_6$ superacids).[11] Albeit the existence of the HSb_3F_{16} superacid has not yet been confirmed experimentally, its deprotonated (*i.e.*, anionic) form $Sb_3F_{16}^-$ is a well-known system which was extensively utilized to create atypical salts and complexes.[40–42]

As indicated above, the theoretical search for novel superacids that have been carried out during last few years led to proposing various promising molecular systems whose usefulness as strong acids is yet to be verified experimentally. In our opinion, however, one important issue was being neglected while performing those investigations employing quantum chemistry methods. Namely, it was preconceived that the number of molecules playing the Brønsted acid role (*e.g.*, HF) is approximately equal to the number of molecules that play the Lewis acid role (*e.g.*, SbF_5, AlF_3) in the mixture that represents a given Lewis–Brønsted superacid. In other words, it was assumed that these both components are combined using 1 : 1 ratio. As a consequence, the simplest 'building block' that was supposed to exhibit the superacid properties was thought of as composed of a single Lewis acid molecule interacting with one Brønsted acid system. Thus, in this contribution we are going to address the issue of the Brønsted/Lewis system acidity in a different way, namely, we intend to verify whether the acidic strength of such species depends on the number of Brønsted acid molecules surrounding a single Lewis acid moiety. Our decision to undertake such a study was motivated by the following observations: (i) the recently reported crystal structures of the HF/AsF_5 ($HAsF_6$)[19] and HF/SbF_5 ($HSbF_6$)[15] superacids clearly show the presence of more than one HF molecule in the vicinity of the Lewis acid unit (either AsF_5 or SbF_5); (ii) earlier experimental studies revealed the existence of various ions (*i.e.*, H_2F^+, $H_3F_2^+$, SbF_6^-) in the liquid HF/SbF_5 ($HSbF_6$);[43–45] and (iii) some superacid preparation procedures describe the use of the excess of anhydrous hydrogen fluoride.[19] Therefore, one might speculate that each Lewis acid molecule may interact with more than one HF moiety in the final superacid mixture. In addition, it seems likely that the mutual interactions among the HF moieties surrounding each Lewis acid molecule contribute to the system's ability to donate a proton. Hence, in order to shed more needed light on this problem, we decided to investigate the gas phase Gibbs free deprotonation energy dependence on the number of hydrogen fluoride molecules surrounding two arbitrarily chosen Lewis acids (*i.e.*, AlF_3 and GeF_4).

2. Methods

The nHF/AlF_3 and nHF/GeF_4 (n = 1–6) closed-shell neutral systems (*i.e.*, AlF_3 and GeF_4 Lewis acids surrounded by n hydrogen fluoride molecules) and their corresponding anions (*i.e.*, negatively charged closed-shell species formed by deprotonation) were investigated using theoretical quantum chemistry methods. In particular, the equilibrium geometries and harmonic vibrational frequencies were calculated using Density Functional Theory (DFT) method with the B3LYP[46,47] functional and the 6-311++G(d,p)[48,49] basis sets. The final electronic energies of all such determined structures were obtained by applying the quadratic configuration interaction method with single and double substitutions (QCISD)[50–52] together with the same 6-311++G(d,p) basis set. The predicted error in estimating deprotonation energy values due to the 6-311++G(d,p) basis set choice was estimated as not exceeding 2 kcal mol^{-1} (which was evaluated by comparing the DE values obtained with the 6-311++G(d,p) and aug-cc-pVTZ basis sets for one representative superacid).

The random search was performed while exploring the configuration space of each nHF/AlF_3 and nHF/GeF_4 (n = 1–6) closed-shell neutral as well as $((n-1)HF/AlF_4)^-$ and $((n-1)HF/GeF_5)^-$ (n = 1–6) closed-shell anionic system. Namely, in the case of neutral systems, various possibilities of attaching the HF molecules to either AlF_3 or GeF_4 were examined by treating them as the starting structures during the independent geometry optimization procedures. In addition, various combinations of mutual interactions among the HF systems were taken into account. In the case of negatively charged systems, our search was mostly based on assuming the presence of a central unit (either AlF_4 or GeF_5) in the structure (as the AlF_4^- or GeF_5^- correspond to very strongly bound anions).

The electronic and Gibbs free energies of the deprotonation reactions (DE and ΔG_{acid}, respectively) were evaluated using the QCISD electronic energies and the zero-point energy corrections, thermal corrections (at T = 298.15 K) and entropy contributions estimated with the B3LYP method and 6-311++G(d,p) basis set (in each case the Gibbs free energy of the proton was also accounted for). The resulting ΔG_{acid} values correspond to the Gibbs free energies characterizing the following processes for ($n = 1 - 6$):

$$n\text{HF/AlF}_3 \rightarrow ((n-1)\text{HF/AlF}_4)^- + \text{H}^+$$

and

$$n\text{HF/GeF}_4 \rightarrow ((n-1)\text{HF/GeF}_5)^- + \text{H}^+.$$

Since the proper evaluation of the thermodynamic properties might be questionable in the case of weakly bound systems, we mainly focus on the deprotonation energies (DE) characterizing the species investigated, whereas the presented Gibbs free deprotonation energies (ΔG_{acid}) should be considered as less reliable and possibly plagued by errors.

The partial atomic charges (q^{ESP}) were fitted to the electrostatic potential according to the Merz–Singh–Kollman scheme.[53]

All calculations were performed using the GAUSSIAN 09 (Rev. A.02) package.[54]

3. Results

3.1. The AlF_3 Lewis acid surrounded by various number of HF molecules

The lowest energy structures of nHF/AlF_3 (n = 1–6) systems are depicted in Fig. 1 whereas the corresponding higher energy

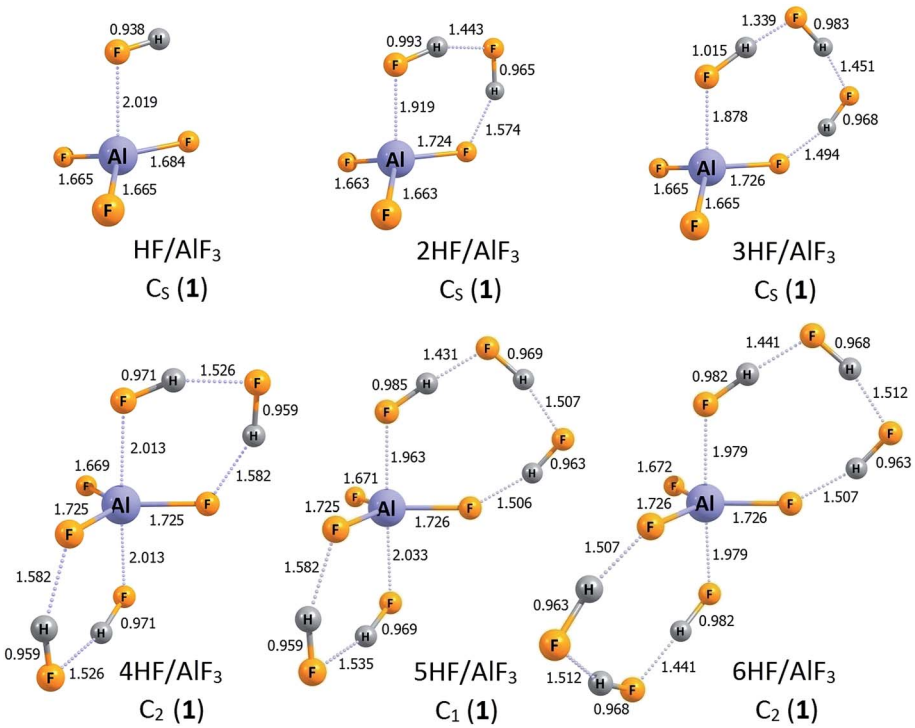

Fig. 1 The structures of the lowest energy isomers of the *n*HF/AlF_3 superacids ($n = 1$–6). Selected bond lengths are given in Å. Dative bonds and hydrogen bonds are represented by the dotted lines.

isomers are shown in Fig. 2. The simplest case of the AlF_3 Lewis acid interacting with one HF molecule, HF/AlF_3 ($HAlF_4$), has already been characterized as a superacid composed of the hydrogen fluoride donating its fluorine's lone pair to the empty Al's 3p atomic orbital of AlF_3 quasi-planar fragment and additionally stabilized by the FH$\cdots$$F_3$Al hydrogen bond.[21,22,28] The DE of 279–280 kcal mol^{-1} and ΔG_{acid} of 267–269 kcal mol^{-1} (depending on the theory level employed)[21,22,28] were predicted for this superacid, however, in this contribution we assume the DE = 279 kcal mol^{-1} and ΔG_{acid} = 267 kcal mol^{-1} values for consistency with the results presented for the remaining *n*HF/AlF_3 ($n = 2$–6) systems. The 2HF/AlF_3 species might be viewed as formed by the attachment of the second HF molecule to the HF/AlF_3 system, hence it resembles the deformed neutral AlF_3 molecule with two HF moieties attached, see structure 2HF/AlF_3 (**1**) in Fig. 1. One HF molecule forms a dative HF $\rightarrow$ AlF_3 bond (1.919 Å) with the AlF_3 whereas the other HF fragment is involved in the formation of two H-bonds. The DE of 278 kcal mol^{-1} and ΔG_{acid} of 264 kcal mol^{-1} were predicted for this system which indicates the decrease of DE by 1 kcal mol^{-1} and the decrease of ΔG_{acid} by 3 kcal mol^{-1} with respect to the HF/AlF_3, see Table 1. In addition, we found two other isomeric structures of 2HF/AlF_3 (see 2HF/AlF_3 (**2**) and 2HF/AlF_3 (**3**) in Fig. 2) having their energy larger by 6–9 kcal mol^{-1} than the lowest energy structure 2HF/AlF_3 (**1**). Interestingly, the structures of these higher energy isomers are qualitatively different, as the isomer 2HF/AlF_3 (**2**) contains two HF molecules localized on the opposite sides of the quasi-planar AlF_3 fragment which allows for the formation of two dative bonds (HF $\rightarrow$ Al(3p) $\leftarrow$ FH) and two H-bonds between HF and AlF_3 fragments, whereas the structure of 2HF/AlF_3 (**3**) contains one HF system forming a dative HF $\rightarrow$ Al(3p) bond with AlF_3 and the second one linked (*via* the H-bond) to the fluorine atom of the central AlF_3 unit, see Fig. 2.

The lowest energy isomer 3HF/AlF_3 (**1**) depicted in Fig. 1 resembles the most stable structure of 2HF/AlF_3 (**1**) with one more HF molecule involved in the resulting three member HF-based bridge whose F-end forms a dative bond with Al's empty 3p atomic orbital while the H-terminus is linked (*via* H-bond) to the F atom of the AlF_3 fragment. It seems important to stress that the H–F bond lengths in three HF molecules span the 0.968–1.015 Å range and the partial atomic charges in each of these HF units sum up to zero which clearly indicates that the whole system is correctly described by the 3HF/AlF_3 formula, see Fig. 1. The acidity of 3HF/AlF_3 (**1**) is slightly stronger than that of 2HF/AlF_3 (**1**) as its DE of 275 kcal mol^{-1} is smaller by 3 kcal mol^{-1} than the corresponding DE characterizing the 2HF/AlF_3 (**1**), see Table 1 (analogous decrease of ΔG_{acid} by 3 kcal mol^{-1} is also observed). We also found two other geometrically stable structures of 3HF/AlF_3 (depicted in Fig. 2 as 3HF/AlF_3 (**2**) and 3HF/AlF_3 (**3**)) having their electronic energies within 6 kcal mol^{-1} with respect to the global minimum. The structure 3HF/AlF_3 (**2**) resembles the 2HF/AlF_3 (**2**) with the additional (third) HF molecule enabling the H-bond connection to the AlF_3 moiety, whereas the structure of 3HF/AlF_3 (**3**) clearly corresponds to the 2HF/AlF_3 (**1**) with the additional HF molecule H-bonded to the fluorine atom of the AlF_3, see Fig. 1 and 2. Again, it appears that all three HF fragments in both 3HF/AlF_3 (**2**) and

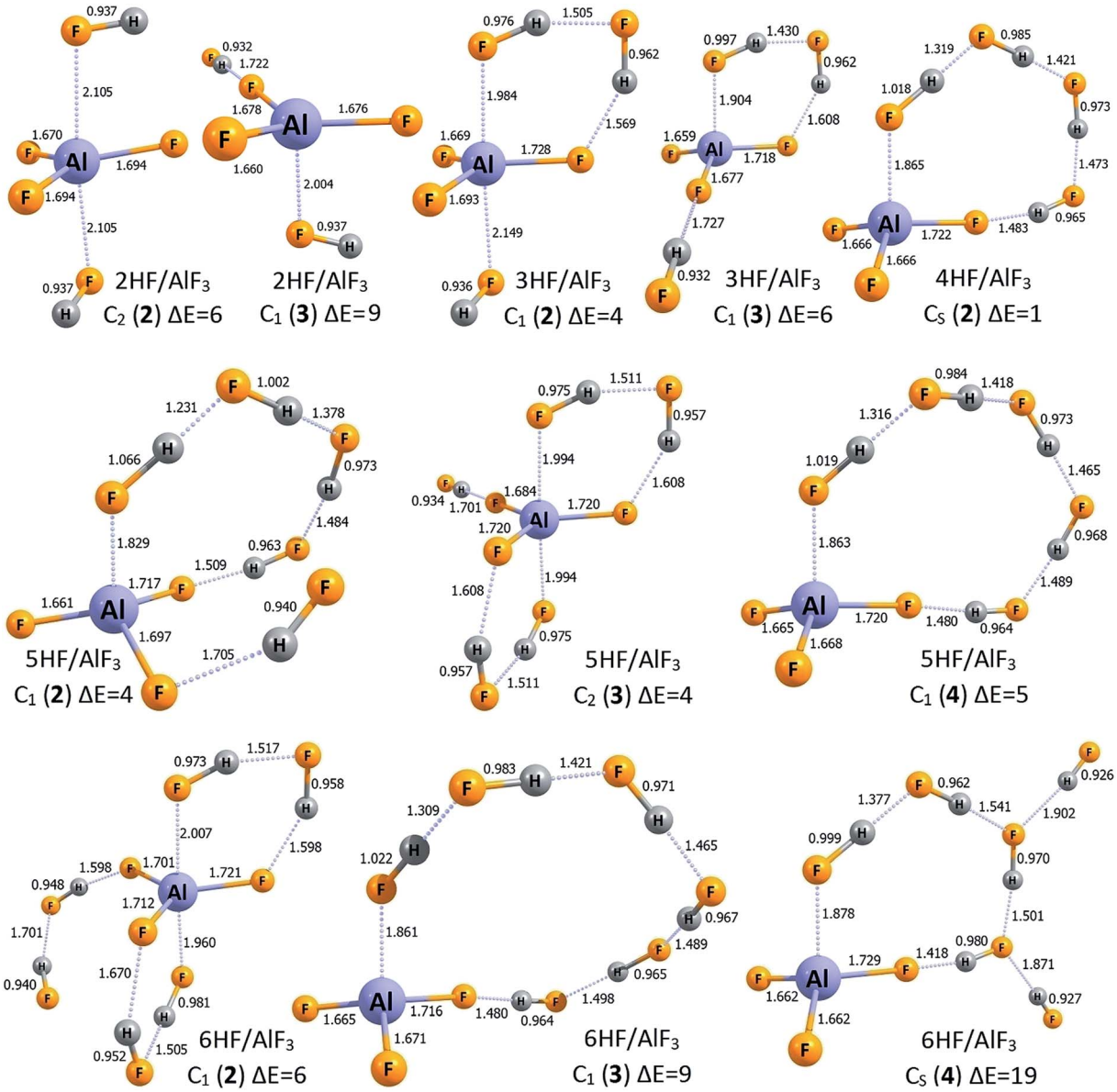

Fig. 2 The structures of the higher energy isomers of the nHF/AlF$_3$ superacids (n = 1–6). Selected bond lengths are given in Å. Relative energies (ΔE) with respect to the corresponding lowest energy isomers are given in kcal mol^{-1}. Dative bonds and hydrogen bonds are represented by the dotted lines.

Table 1 The deprotonation energies (DE) and Gibbs free deprotonation energies (ΔG_{acid}, for T = 298.15 K) predicted for the lowest energy isomers of the nHF/AlF$_3$ superacids (for n = 1–6). The $T\Delta S$ term (for T = 298.15 K) is separated from ΔG_{acid}. All numbers are given in kcal mol^{-1}

Species	Symmetry	DE	$T\Delta S$	ΔG_{acid}
HF/AlF$_3$	C_s	279.2	6.3	267.4
2HF/AlF$_3$	C_s	277.8	8.6	264.3
3HF/AlF$_3$	C_s	274.6	9.6	260.8
4HF/AlF$_3$	C_2	270.5	12.8	253.1
5HF/AlF$_3$	C_1	268.9	13.4	251.3
6HF/AlF$_3$	C_2	270.4	15.3	251.1

3HF/AlF$_3$ (**3**) are typical hydrogen fluoride systems with their vanishing net partial atomic charges and 0.932–0.997 Å bond lengths.

The lowest energy structure of 4HF/AlF$_3$ (depicted in Fig. 1 as 4HF/AlF$_3$ (**1**)) mimics a trigonal bipyramid AlF$_5$ having two elongated (2.013 Å) F → Al dative bonds and three shorter (1.669–1.725 Å) covalent Al–F bonds (in the planar AlF$_3$ fragment) whose fluorine ligands are connected *via* the H-bond networks. However, taking into account the bond lengths and partial atomic charges (summing up to zero for each of four HF fragments), one should consider this system as the AlF$_3$ and four HF molecules assembled together (rather than, for instance, composed of the AlF_5^{2-} dianion and two H_2F^+

cations). As far as the acidity of the 4HF/AlF_3 (**1**) is concerned, we predicted the DE of 271 kcal mol^{-1} (ΔG_{acid} = 253 kcal mol^{-1}), which indicates that the acidic strength of this system should be even larger than the acidity of AlF_3 surrounded by a smaller number (from 1 to 3) HF molecules, see Table 1. We also found one higher energy isomer of this species (depicted in Fig. 2 as 4HF/AlF_3 (**2**)) whose relative energy is larger by only 1 kcal mol^{-1}. Such a quasi-degeneracy clearly indicates that both of these structures (*i.e.*, **1** and **2** of 4HF/AlF_3) should be present in the bulk. The isomer 4HF/AlF_3 (**2**), however, possesses a different structure than 4HF/AlF_3 (**1**), as it corresponds to the quasi-planar AlF_3 unit whose Al atom and F atom are connected with the $(HF)_4$ H-bonded linkage (analogously to the global minimum of 3HF/AlF_3 where similar $(HF)_3$ internally H-bonded linkage is present, see 3HF/AlF_3 (**1**) in Fig. 1). In addition, the conclusion about the presence of the AlF_3 and four HF units formulated for the structure 4HF/AlF_3 (**1**) (*i.e.*, indicating the absence of H_2F^+ cations) remains valid also for the competitive isomer 4HF/AlF_3 (**2**), hence justifying its 4HF/AlF_3 formula.

While investigating the AlF_3 Lewis acid surrounded by five HF molecules, 5HF/AlF_3, we found the lowest energy structure 5HF/AlF_3 (**1**) (depicted in Fig. 1) and three higher energy isomers (shown in Fig. 2 as isomers **2**, **3**, and **4**). The global minimum 5HF/AlF_3 (**1**) resembles the lowest energy isomer 4HF/AlF_3 (**1**) as it also contains a trigonal bipyramid AlF_5 with two elongated (1.963–2.033 Å) F → Al dative bonds and three shorter (1.671–1.726 Å) covalent Al–F bonds (in the planar AlF_3 fragment) whose F ligands are linked *via* the H-bonded units. However, as it was observed and discussed for 4HF/AlF_3 (**1**) (see the preceding paragraph), the more proper way of viewing this system is that consistent with the 5HF/AlF_3 formula, as neither AlF_5^{2-} dianion nor H_2F^+ cations are present (as it might have been expected when distinguishing the AlF_5 core as the independent fragment of the structure). Such a conclusion is supported by the typical (0.959–0.985 Å) lengths of H–F bonds in all five HF moieties and their vanishing net atomic partial charges (*i.e.*, atomic partial charges in each HF fragment sum up to zero and this is also the case for the remaining AlF_3 fragment), see Fig. 1. The DE of 269 kcal mol^{-1} was predicted for 5HF/AlF_3 (**1**) which means the 2 kcal mol^{-1} decrease in comparison to 4HF/AlF_3 (**1**), see Table 1. Certainly, it should result in a slightly stronger acidity of the former compound, however the reported DE drop seems rather small. As far as the higher energy isomers of 5HF/AlF_3 are concerned, the three remaining isomers shown in Fig. 2 possess their relative energies within 4–5 kcal mol^{-1} and thus they might be considered as competitive. The structure of 5HF/AlF_3 (**2**) resembles that of 4HF/AlF_3 (**2**) with the additional HF molecule attached to the different fluorine atom of AlF_3 unit, the structure of 5HF/AlF_3 (**3**) bears a similar resemblance to the 4HF/AlF_3 (**1**), whereas the structure of 5HF/AlF_3 (**4**) is composed of the AlF_3 fragment whose only two F atoms are involved in the connections to the HF molecules (alike it was observed for 2HF/AlF_3 (**1**), 3HF/AlF_3 (**1**), and 4HF/AlF_3 (**2**)), however, the $(HF)_n$ internally H-bonded linkage consists of five HF molecules in the 5HF/AlF_3 (**4**) case, see Fig. 1 and 2.

Finally, the lowest energy structure of 6HF/AlF_3 (depicted as 6HF/AlF_3 (**1**) in Fig. 1) is similar to the most stable isomer of 5HF/AlF_3 (**1**). Namely, the planar AlF_3 central fragment interacts with two $(HF)_3$ internally H-bonded moieties, each of which forms (using its F-end) the dative F → Al(3p) bond and the hydrogen H···F–AlF_2 bond (utilizing its H-terminus) with the AlF_3 core. Again, viewing the 6HF/AlF_3 (**1**) structure as composed of negatively charged AlF_5^{2-} core, two H_2F^+ cations and two neutral HF molecules interacting with one another seems not justified. Instead, the interatomic distances and the results of the population analysis clearly indicate that this system represents the neutral AlF_3 fragment interacting with six HF molecules (the mutual interactions among the HF systems are also present) and thus describing the resulting species by the 6HF/AlF_3 formula is adequate. The gas phase acidity of 6HF/AlF_3 (**1**), manifested by DE of 270 kcal mol^{-1}, seems very similar to that predicted for the system having one HF molecule less (5HF/AlF_3 (**1**)). Namely, the difference in DE for these two species does not exceed 1.5 kcal mol^{-1} (see Table 1). We view this result as very important because it shows that the addition of the sixth HF molecule to the 5HF/AlF_3 system does not change its acidity, and thus the saturation of both DE and ΔG_{acid} seems achieved (further discussion of the consequences of this result is provided in the closing section). We have also found three higher energy isomers of 6HF/AlF_3 having their relative energies in the 6–19 kcal mol^{-1} range (with respect to the global minimum 6HF/AlF_3 (**1**)), see structures 6HF/AlF_3 (**2**, **3**, and **4**) depicted in Fig. 2. However, we believe that only one of them (6HF/AlF_3 (**2**) whose structure resembles that of 5HF/AlF_3 (**3**) with one more HF unit attached) might be considered as competitive with 6HF/AlF_3 (**1**) because the relative energies of 6HF/AlF_3 (**3**) and 6HF/AlF_3 (**4**) seem too large (*i.e.*, 9 and 19 kcal mol^{-1}, respectively).

Having discussed the structures and acidities of the *n*HF/AlF_3 (*n* = 1–6) systems (including their isomers possessing relative energies within 20 kcal mol^{-1}), we present the lowest energy anionic structures of $((n-1)HF/AlF_4)^-$ (*n* = 1–6) that are the resulting compounds of the *n*HF/AlF_3 deprotonation. The equilibrium anionic structures are depicted in Fig. 3. One may notice that the AlF_4 structural unit can be distinguished in all of these negatively charged systems, moreover, the population analysis and tetrahedral-like geometry of that AlF_4 fragment indicate that the entire excess electron density is delocalized over its fluorine ligands. Thus, each $((n-1)HF/AlF_4)^-$ anion (*n* = 1–6) is in fact composed of the quasi-tetrahedral AlF_4^- core and a certain number of HF molecules bound to its F ligands *via* the H-bonds. The symmetry of the resulting structures seems enforced by the number of the HF molecules attached, namely, the T_d-symmetry corresponds to the AlF_4^- surrounded by either zero or four HF moieties, C_{3v}-symmetry is achieved for either one or three HF molecules, whereas the C_{2v}-symmetry anionic structure is observed when two HF systems are coordinated. Clearly, the presence of four electronegative ligands in the AlF_4^- anion indicates that this negatively charged species can be maximally stabilized by four HF molecules whereas the fifth hydrogen fluoride system remains outside this first coordination sphere (compare the structures of $(4HF/AlF_4)^-$ and (5HF/

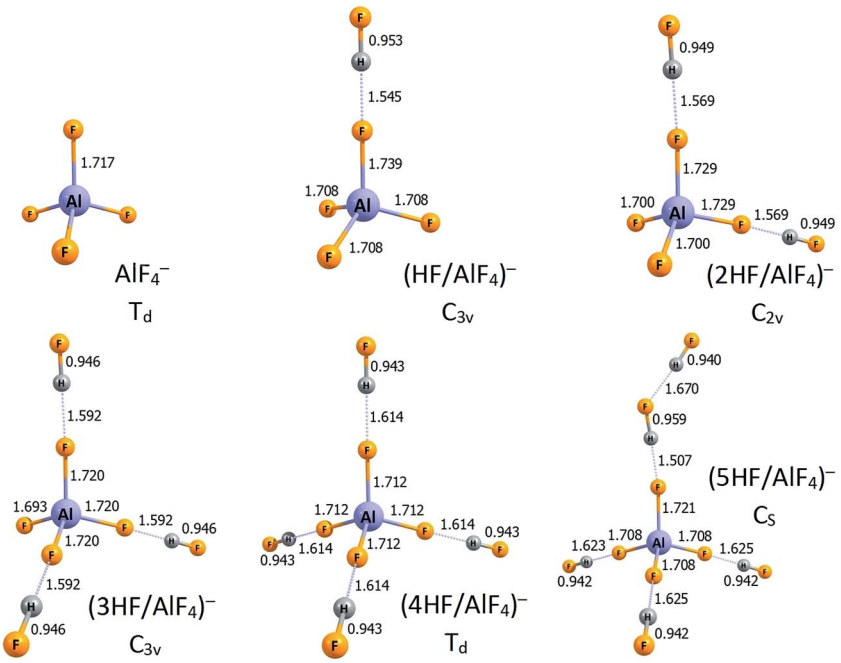

Fig. 3 The structures of the lowest energy isomers of the $((n-1)HF/AlF_4)^-$ anions ($n = 1$–6). Selected bond lengths are given in Å. Hydrogen bonds are represented by the dotted lines.

$AlF_4)^-$ anions in Fig. 3). Thus the lowest value of deprotonation energy (DE = 268.9 kcal mol^{-1}, see Table 1) for the nHF/AlF_3 superacids ($n = 1$–6) corresponds to the 5HF/AlF_3 system while the effect of attaching an additional HF molecule is nearly marginal. Such an observation indicates the key role of microsolvation of an anionic species in the deprotonation process and its influence on the change in energy (with respect to the neutral microsolvated system).

3.2. The GeF_4 Lewis acid surrounded by various number of HF molecules

The lowest energy structures of nHF/GeF_4 ($n = 1$–6) systems and the corresponding higher energy isomers are depicted in Fig. 4 and 5, respectively. The structurally simplest HF/GeF_4 system (*i.e.*, the GeF_4 Lewis acid interacting with one hydrogen fluoride molecule) has already been characterized as a promising superacid consisting of the HF fragment donating its F's lone pair to the empty germanium's 4p atomic orbital of the GeF_4 quasi-tetrahedral unit.[28] The DE of 295 kcal mol^{-1} and ΔG_{acid} of 285 kcal mol^{-1} predicted for HF/GeF_4 (see Table 2) are in good agreement with the earlier estimations obtained at a different theory level.[28] The lowest energy structure of 2HF/GeF_4 is assembled in a similar way, with one additional HF molecule attached, which results in the formation of two hydrogen bonds and in the shortening (by 0.22 Å) of the HF → Ge(4p) dative bond (in comparison to the HF/GeF_4), see Fig. 4. The deprotonation energy estimated for the 2HF/GeF_4 is smaller by 8 kcal mol^{-1} than that predicted for HF/GeF_4, see Table 2, which indicates considerably stronger acidity of the former species. It seems important to notice that the DE drop observed for HF/GeF_4 upon the second HF molecule addition is much larger than the analogous DE decrease noted for the HF/AlF_3, see the preceding section. We also found another isomeric structure of 2HF/GeF_4 (see 2HF/GeF_4 (**2**) in Fig. 5) whose energy is larger by only 4 kcal mol^{-1} than the energy of global minimum 2HF/GeF_4 (**1**). Similarly to the higher energy isomer of 2HF/AlF_3 (**2**) (see Fig. 2), the structure of 2HF/GeF_4 (**2**) might be described as two HF molecules attached to the opposite sides of the GeF_4 central unit which allows for the formation of one dative bond (HF → Ge(4p)) and one hydrogen bond between HF and GeF_4 fragments, see Fig. 5.

The lowest energy structures of GeF_4 interacting with three (3HF/GeF_4 (**1**)), four (4HF/GeF_4 (**1**)), five (5HF/GeF_4 (**1**)), and six (6HF/GeF_4 (**1**)) hydrogen fluoride molecules follow the same general pattern, see Fig. 4. Namely, in each of these systems, the internally H-bonded HF-chain ($(HF)_n$) acts as a molecular "clasp" having two different ends – one of them (F-terminus) is involved in the $(HF)_n$ → Ge(4p) dative bond formation while the other (H-terminus) forms a hydrogen bond with one of the fluorine ligands the central tetrahedral-like GeF_4 unit is decorated with. In the case of the 6HF/GeF_4 (**1**), however, the $(HF)_6$ clasp is long enough to attach its H-end to the fluorine ligand localized on the opposite side of the GeF_4 fragment (with respect to the dative bond), see Fig. 4, which in turn allows for additional stabilization coming from the interaction of another F ligand with the hydrogen atoms of the $(HF)_6$ chain. In each of the nHF/GeF_4 (**1**) ($n = 1$–6) structures one may easily distinguish the central GeF_4 unit having its four fluorine atoms localized in a quasi-tetrahedral manner around the Ge atom. On the other hand, it might be tempting to consider these structures as consisting of the GeF_5 unit (forming a deformed trigonal bipyramid) – if such a view were applied, however, it would have

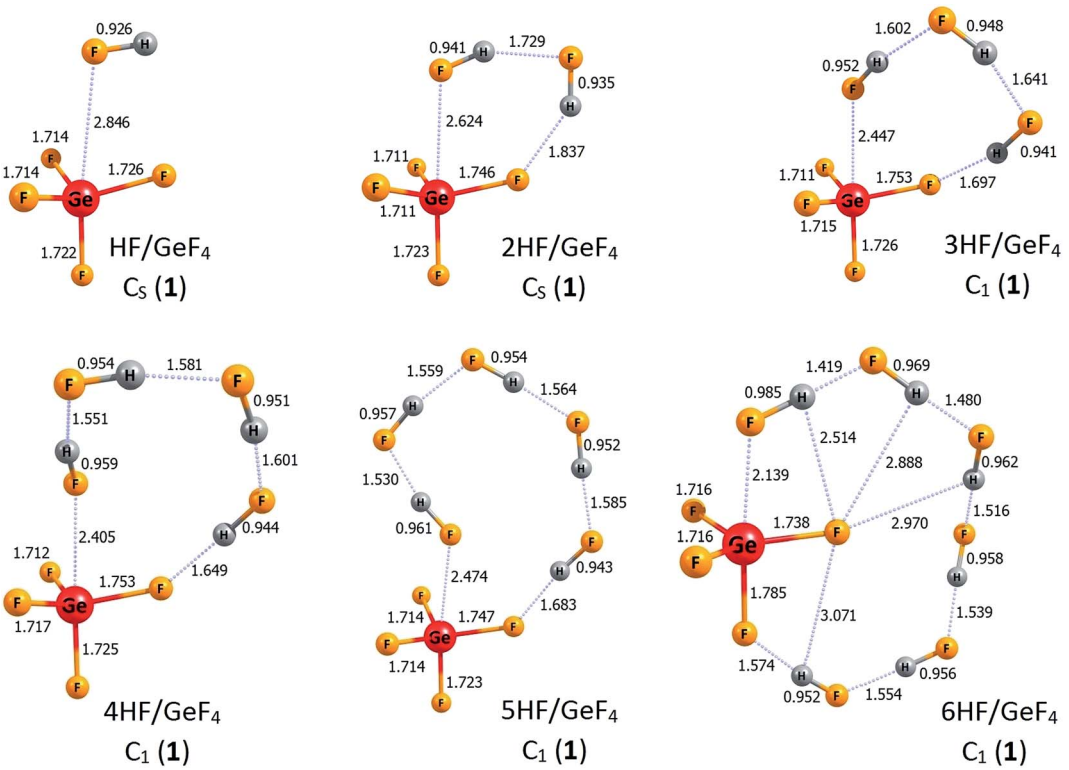

Fig. 4 The structures of the lowest energy isomers of the *n*HF/GeF_4 superacids ($n = 1$–6). Selected bond lengths are given in Å. Dative bonds and hydrogen bonds are represented by the dotted lines.

required the presence of at least one H_2F (likely cationic) moiety in the remaining fragment. As we verified (by analyzing the interatomic distances and partial atomic charges), such a treatment is not justified, mainly because all the H–F bond lengths are typical for HF molecules (0.93–0.99 Å), one F atom forms a significantly elongated bond with the Ge atom, and the partial atomic charges sum up to approximately zero for each HF fragment in the *n*HF/GeF_4 (**1**) ($n = 1$–6) structures, see Fig. 4. Hence, we conclude that these lowest energy isomeric structures consist of the GeF_4 (rather than GeF_5 or GeF_6) tetrahedral-like unit and the HF molecules attached, whereas the H_2F^+ fragments are absent.

The description of the *n*HF/GeF_4 ($n = 3$–6) systems would not be complete if the higher energy isomeric structures were neglected. Hence, in Fig. 5 we present two additional isomers of 3HF/GeF_4, one higher energy isomer of 4HF/GeF_4, three isomeric structures of 5HF/GeF_4, and three higher energy isomers of 6HF/GeF_4. The relative energies of 3HF/GeF_4 (**2**) and 3HF/GeF_4 (**3**) (calculated as equal to 5 and 18 kcal mol^{-1}, respectively) indicate that only the isomer **2** may compete with the 3HF/GeF_4 (**1**) global minimum. The structure of 3HF/GeF_4 (**2**) resembles that of 2HF/GeF_4 (**1**) with the additional HF molecule attached to the opposite side of the GeF_4, whereas the higher energy isomer 3HF/GeF_4 (**3**) contains the quasi-planar GeF_4 fragment (whose atypical structure is likely caused by the formation of two (instead of one) dative bonds), see Fig. 5. It seems also important to note that each of three HF molecules attached to this GeF_4 fragment in 3HF/GeF_4 (**3**) remains nearly intact. The attachment of four HF molecules to GeF_4 leads to only one higher energy isomer (within 20 kcal mol^{-1}) depicted in Fig. 5 (4HF/GeF_4 (**2**)). The structure of 4HF/GeF_4 (**2**) contains a quasi-planar GeF_4 fragment forming two dative bonds and two hydrogen bonds with two $(HF)_2$ clasps that link the ligands on the opposite sides, however, its energy is 12 kcal mol^{-1} higher than that of 4HF/GeF_4 (**1**) and thus the formation of 4HF/GeF_4 (**2**) isomer is not likely at low temperatures. The situation is different for the 5HF/GeF_4 systems, namely, the relative energies of all three higher energy isomers (*i.e.*, 5HF/GeF_4 (**2**, **3**, and **4**)) are rather small (not exceeding 8 kcal mol^{-1}) with respect to the global minimum **1**, hence they may compete with the lowest energy isomer. The structures of 5HF/GeF_4 consist of either a quasi-tetrahedral (**2** and **3**) or quasi-planar (**4**) GeF_4 unit surrounded by five HF molecules in various ways, see Fig. 5. Finally, the relative energies of two (**2** and **3**) higher energy isomers of 6HF/GeF_4 are small enough (3–6 kcal mol^{-1}) to allow for their presence at low temperatures, while the energy of 6HF/GeF_4 (**4**) was calculated to be 11 kcal mol^{-1} larger than that of 6HF/GeF_4 (**1**). The structures of 6HF/GeF_4 (**3**) and 6HF/GeF_4 (**4**) contain a quasi-planar GeF_4 fragment allowing for the formation of two dative bonds whereas the structure of 6HF/GeF_4 (**2**) consists of a tetrahedral-like GeF_4 moiety linked *via* one dative bond with the HF molecule localized nearby, see Fig. 5. Even though the structures of 6HF/GeF_4 (**3**) and 6HF/GeF_4 (**4**) might suggest the presence of the GeF_6^{2-} fragment (which in turn would enforce the presence of two H_2F^+ fragments), we verified that such a supposition is not justified. As it was already discussed for the

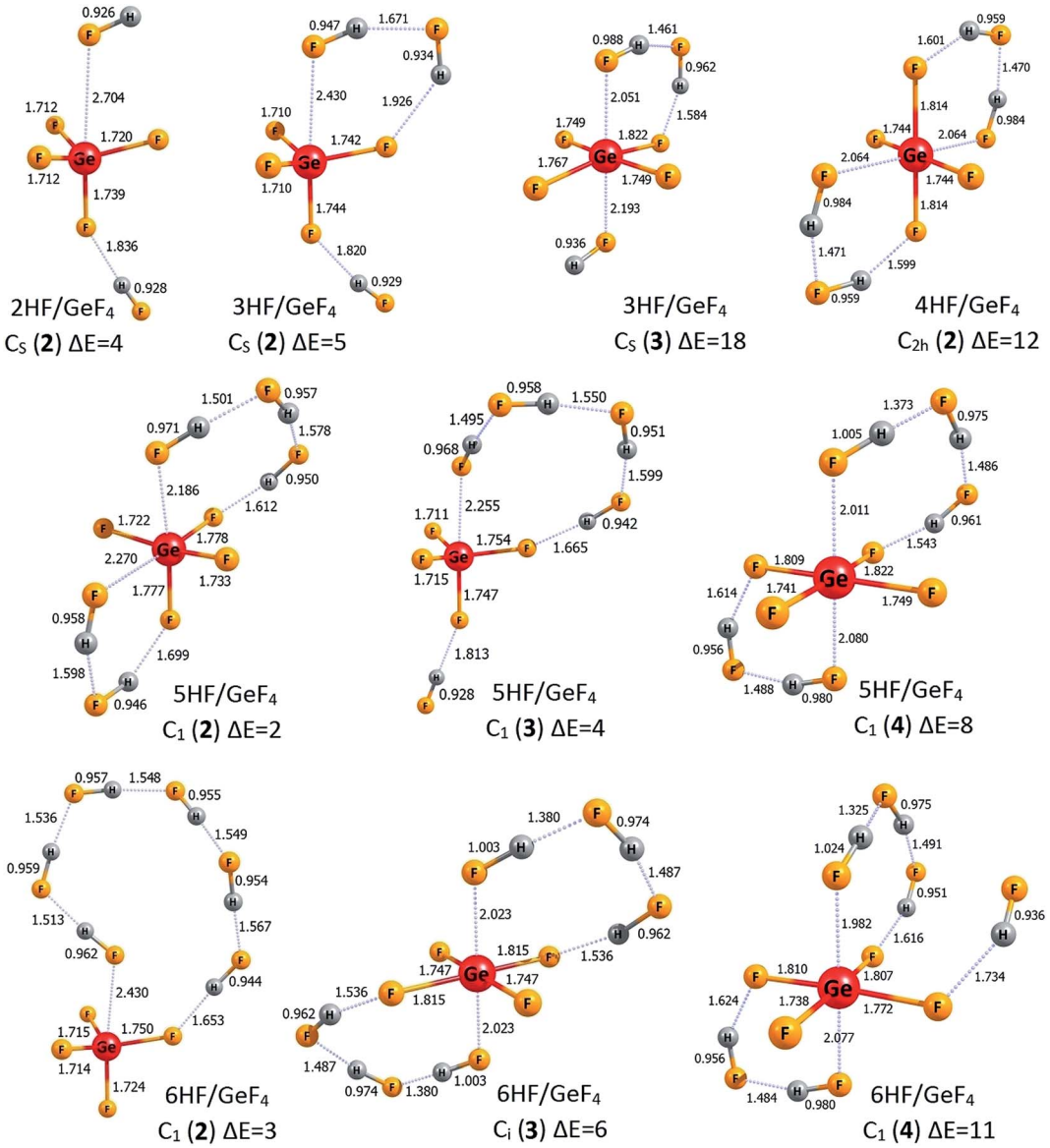

Fig. 5 The structures of the higher energy isomers of the nHF/GeF$_4$ superacids (n = 1–6). Selected bond lengths are given in Å. Relative energies (ΔE) with respect to the corresponding lowest energy isomers are given in kcal mol^{-1}. Dative bonds and hydrogen bonds are represented by the dotted lines.

Table 2 The deprotonation energies (DE) and Gibbs free deprotonation energies (ΔG_{acid}, for T = 298.15 K) predicted for the lowest energy isomers of the nHF/GeF$_4$ superacids (for n = 1–6). The $T\Delta S$ term (for T = 298.15 K) is separated from ΔG_{acid}. All numbers are given in kcal mol^{-1}

Species	Symmetry	DE	$T\Delta S$	ΔG_{acid}
HF/GeF$_4$	C_s	294.8	4.1	285.0
2HF/GeF$_4$	C_s	286.9	7.4	273.7
3HF/GeF$_4$	C_1	281.4	8.5	267.2
4HF/GeF$_4$	C_1	278.1	9.7	262.7
5HF/GeF$_4$	C_1	276.1	10.8	259.8
6HF/GeF$_4$	C_1	277.6	13.6	259.5

other structures, the interatomic distances in 6HF/GeF$_4$ (**3**) and 6HF/GeF$_4$ (**4**) indicate that all HF fragments resemble typical hydrogen fluoride molecules (with their H–F bond lengths spanning the 0.94–1.02 Å range) involved in the formation of various H-bonded structures rather than the cationic H_2F^+ fragments (such a conclusion is also additionally supported by the results of the population analysis showing approximately zero net charges on each HF molecule).

According to the nHF/AlF$_3$ (n = 1–6) description provided in the preceding section, we briefly comment on the anionic structures of the nHF/GeF$_4$ (n = 1–6) superacids (*i.e.*, the corresponding anionic systems that result from deprotonation of those compounds). As for the $((n-1)HF/AlF_4)^-$ anions (n = 1–6), we limit our discussion to the lowest energy anionic isomers $((n-1)HF/GeF_5)^-$ anions (n = 1–6), while their excess electron

detachment energies are not considered here (although we verified that all the presented anions are electronically stable systems). The lowest energy $((n-1)HF/GeF_5)^-$ anionic structures are depicted in Fig. 6. In each case, the GeF_5 structural unit can be distinguished with five F ligands forming a trigonal bipyramid around the germanium atom. The population analysis indicate that the GeF_5 fragment holds the entire excess electron density in these anions (more precisely, the excess negative charge is delocalized over five fluorine ligands in GeF_5). Thus, each of these negatively charged systems (*i.e.*, $((n-1)HF/GeF_5)^-$) should be considered as the GeF_5^- anion with the $(n-1)$ hydrogen fluoride molecules attached. As depicted in Fig. 6, in all cases except $(5HF/GeF_5)^-$, the HF molecules are tethered to different fluorine ligands of GeF_5^-. Similarly to the $((n-1)HF/AlF_4)^-$ species (n = 1–6) described in the preceding section, it turns out that the number of ligands in the GeF_5^- anion (whose presence as a central unit was confirmed in all $((n-1)HF/GeF_5)^-$ cases) is crucial regarding its possible microsolvation by HF molecules. Namely, for the increasing value of n, the HF moieties are successively attached to different fluorine atoms that the GeF_5^- central unit consists of (with the only exception of $(5HF/GeF_5)^-$ in which one F ligand is not involved, see Fig. 6). Again, this confirms the crucial role of microsolvation of an anionic species in the overall deprotonation process which manifests itself by the lowest values of deprotonation energy found for the $5HF/GeF_4$ and $6HF/GeF_4$ systems, see Table 2.

As far as the DE and ΔG_{acid} values of the nHF/GeF_4 (n = 3–6) species are concerned, a gradual decrease of the deprotonation energy (accompanied by the Gibbs free deprotonation energy change) is observed when n develops from 3 to 5, see Table 2. The addition of the third HF molecule (resulting in the formation of $3HF/GeF_4$ (**1**)) leads to the DE = 281 kcal mol^{-1}, while introducing fourth and fifth HF fragment lowers DE by another 3 and 2 kcal mol^{-1}, respectively. Finally, we observe that the addition of the sixth hydrogen fluoride molecule has an opposite (although rather small) impact on the acidity, as it causes the deprotonation energy to increase by 1.5 kcal mol^{-1}. As indicated in the preceding paragraph, the described DE (and thus ΔG_{acid}) decrease is mainly caused by the ability of the central GeF_5^- unit to utilize its ligands to successively attach the HF molecules. The consequences of these findings are discussed in the following section.

3.3. Deprotonation energies of the nHF/AlF$_3$ and nHF/GeF$_4$

Although the energies of the deprotonation process for each investigated superacid were already briefly mentioned in the previous sections, we would like to summarize these results and formulate some important conclusions concerning the acidic strength. In general, the DE values calculated for the nHF/AlF$_3$ and nHF/GeF$_4$ (n = 1–6) gathered in Tables 1 and 2 indicate that the acidity strength increases with the increasing number (n) of HF molecules involved. It is manifested by the drop of the DE values (by 9 kcal mol^{-1} for nHF/AlF$_3$ and by 19 kcal mol^{-1} for nHF/GeF$_4$) with n developing from 1 to 5. In both cases, the attachment of the sixth HF molecule does not lead to the further

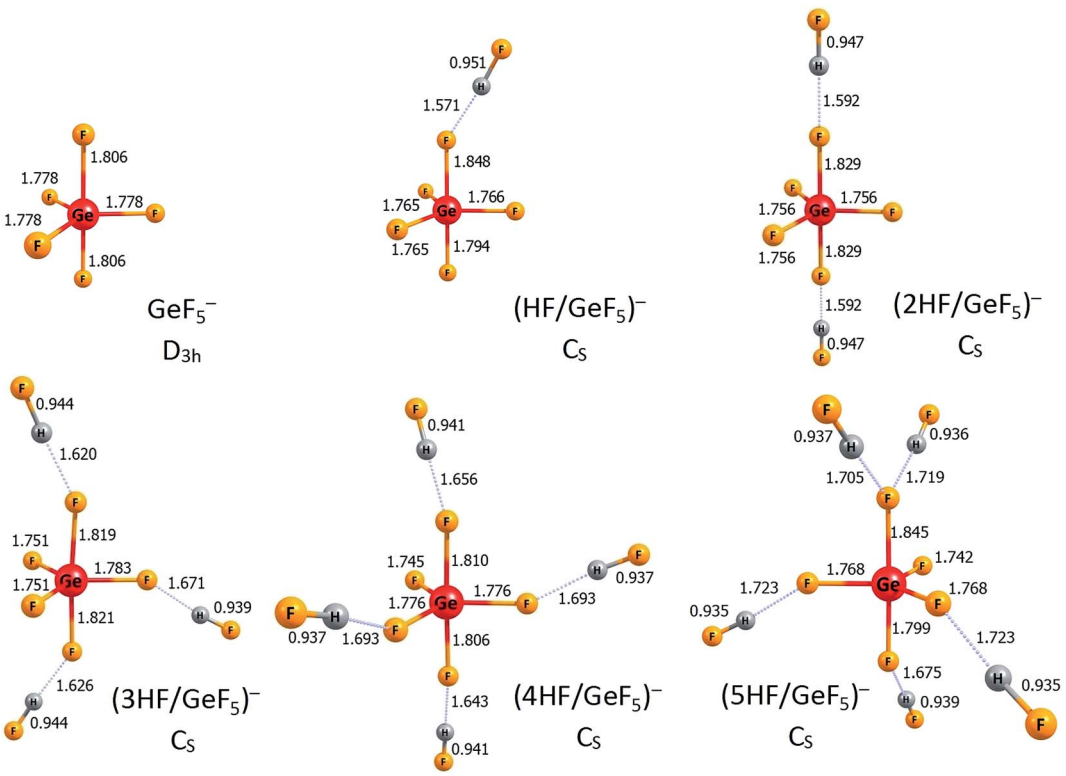

Fig. 6 The structures of the lowest energy isomers of the $((n-1)HF/GeF_5)^-$ anions (n = 1–6). Selected bond lengths are given in Å. Hydrogen bonds are represented by the dotted lines.

acidity increase. The estimated deprotonation energies (depicted in Fig. 7) seem to converge to some limiting values of *ca.* 269–270 kcal mol^{-1} (for *n*HF/AlF_3) and 276–277 kcal mol^{-1} (for *n*HF/GeF_4), see Tables 1 and 2. These deprotonation energy changes are accompanied by the similar ΔG_{acid} changes whose values converge to 251 kcal mol^{-1} (for 6HF/AlF_3) and 260 kcal mol^{-1} (for 6HF/GeF_4).

The results described above suggest that the successive attachment of HF molecules to either AlF_3 or GeF_4 results in a gradual increase of the acidity strength. This acidity strength increase is less and less visible for growing number of HF molecules which leads to the saturation of the DE and ΔG_{acid} values. The saturation of deprotonation energy for both *n*HF/AlF_3 and *n*HF/GeF_4 superacids is likely caused by the limited ability of the AlF_4^- and GeF_5^- anions to attach HF molecules while forming their first coordination spheres. Taking into account that the number of HF molecules introduced (*i.e.*, up to 6) is larger than the number of electronegative sites in either AlF_4^- and GeF_5^- anion, we believe that such a saturation is achieved for both the *n*HF/AlF_3 and *n*HF/GeF_4 series (n = 1–6). Certainly, the slower DE saturation process for *n*HF/GeF_4 than for *n*HF/AlF_3 is caused by the larger number of accessible fluorine ligands in GeF_5^- where the surrounding HF molecules can be attached to. Hence, we speculate that our final limiting DE and ΔG_{acid} values (DE = 269–270 kcal mol^{-1}, ΔG_{acid} = 251 kcal mol^{-1} for *n*HF/AlF_3 and DE = 276–277 kcal mol^{-1}, ΔG_{acid} = 260 kcal mol^{-1} for *n*HF/GeF_4) are reasonable and reliable approximations of the true gas phase deprotonation energies of these superacids (assuming that such superacids are prepared by combining either AlF_3 or GeF_4 Lewis acid with the excess of anhydrous hydrogen fluoride).

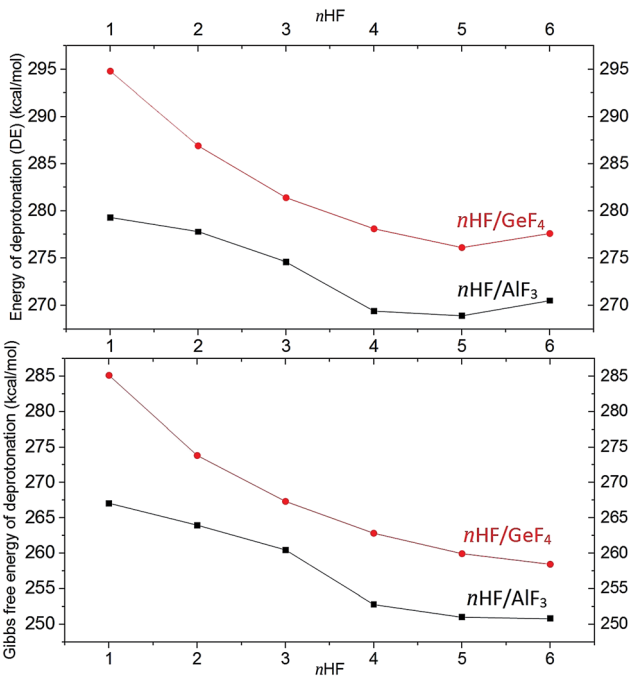

Fig. 7 Deprotonation energies (top) and the Gibbs free deprotonation energies (bottom) (in kcal mol^{-1}) for *n*HF/AlF_3 (black squares) and *n*HF/GeF_4 (red circles) superacids (n = 1–6).

4. Conclusions

On the basis of our quantum chemical calculations performed at the QCISD/6-311++G(d,p)//B3LYP/6-311++G(d,p) level for the *n*HF/AlF_3 and *n*HF/GeF_4 (n = 1–6) neutral superacids (*i.e.*, AlF_3 and GeF_4 Lewis acids surrounded by n hydrogen fluoride (Brønsted acid) molecules) and their corresponding anions (*i.e.*, negatively charged systems formed by deprotonation of the *n*HF/AlF_3 and *n*HF/GeF_4) we formulated the following conclusions:

(i) The acidic strength of the Brønsted/Lewis superacids (approximated here by the deprotonation energies, DE) prepared by combining the Lewis acid with the excess of Brønsted acid should not be estimated by assuming a single Lewis acid molecule interacting with one Brønsted acid molecule as a building block.

(ii) Each Lewis acid moiety is capable of interacting (dative bond and hydrogen bond formation) with more than one Brønsted acid molecule, as verified for AlF_3 and GeF_4 Lewis acids surrounded by various number (from 1 to 6) hydrogen fluoride molecules.

(iii) The successive attachment of HF molecules to either AlF_3 or GeF_4 gradually increases their acidity strength (manifested by the DE decrease) which leads to the saturation of the DE value achieved for the *n*HF/AlF_3 and *n*HF/GeF_4 superacids for n = 5–6.

(iv) The microsolvation of an anionic species generated in the course of a deprotonation reaction (*i.e.*, either AlF_4^- or GeF_5^-) plays a key role in the process as it influences the change in energy with respect to the neutral microsolvated species.

(v) The final values of the deprotonation energies estimated here for the Brønsted/Lewis superacids prepared by combining either AlF_3 or GeF_4 Lewis acids with the excess of anhydrous hydrogen fluoride are equal to 269–270 kcal mol^{-1} and 276–277 kcal mol^{-1}, respectively.

Although our conclusions were formulated by investigating only two arbitrarily chosen Brønsted/Lewis superacids we believe they should be more general in a sense that they might be extended to cover all such superacids prepared in the similar way. Thus the future theoretical predictions of the gas phase acidity of Brønsted/Lewis superacids cannot be limited to evaluating the properties of a building block assumed as a single Lewis acid molecule interacting with one Brønsted acid molecule.

Acknowledgements

This research was supported by the Polish Ministry of Science and Higher Education grant No. DS 530-8376-D499-15 and by the grant no. PSPB-051/2010 from Switzerland through the Swiss Contribution to the enlarged European Union (to P. S.). The calculations have been carried out using resources provided by Wroclaw Centre for Networking and Supercomputing (http://wcss.pl) grant No. 350.

References

1 R. J. Gillespie and T. E. Peel, *Adv. Phys. Org. Chem.*, 1971, **9**, 1–24.

2 R. J. Gillespie and T. E. Peel, *J. Am. Chem. Soc.*, 1973, **95**, 5173–5178.
3 N. F. Hall and J. B. Conant, *J. Am. Chem. Soc.*, 1927, **49**, 3047–3061.
4 G. A. Olah and J. Lukas, *J. Am. Chem. Soc.*, 1967, **89**, 2227–2228.
5 A. F. Bickel, C. J. Gaasbeek, H. Hogeveen, J. M. Oelderik and J. C. Platteeuw, *J. Chem. Soc., Chem. Commun.*, 1967, **13**, 634–635.
6 H. Hogeveen and A. F. Bickel, *J. Chem. Soc., Chem. Commun.*, 1967, **13**, 635–636.
7 G. A. Olah and R. H. Schlosberg, *J. Am. Chem. Soc.*, 1968, **90**, 2726–2727.
8 H. Hogeveen and A. F. Bickel, *Recl. Trav. Chim. Pays-Bas*, 1969, **88**, 371–378.
9 G. A. Olah, Y. Halpern, J. Shen and Y. K. Mo, *J. Am. Chem. Soc.*, 1971, **93**, 1251–1256.
10 A. H. Otto, T. Steiger and S. Schrader, *Chem. Commun.*, 1998, **3**, 391–392.
11 I. A. Koppel, P. Burk, I. Koppel, I. Leito, T. Sonoda and M. Mishima, *J. Am. Chem. Soc.*, 2000, **122**, 5114–5124.
12 K. E. Gutowski and D. A. Dixon, *J. Phys. Chem. A*, 2006, **110**, 12044–12054.
13 A. K. Srivastava and N. Misra, *Polyhedron*, 2015, **102**, 711–714.
14 J. Axhausen, C. Ritter, K. Lux and A. Kornath, *Z. Anorg. Allg. Chem.*, 2013, **639**, 65–72.
15 C. Bour, R. Guillot and V. Gandon, *Chem.–Eur. J.*, 2015, **21**, 6066–6069.
16 G. A. Olah, G. K. Prakash and J. Sommer, *Science*, 1979, **206**, 13–20.
17 D. Touiti, R. Jost and J. Sommer, *J. Chem. Soc., Perkin Trans.*, 1986, **2**, 1793–1797.
18 R. Jost and J. Sommer, *Rev. Chem. Intermed.*, 1988, **9**, 171–199.
19 J. Axhausen, K. Lux and A. Kornath, *Angew. Chem., Int. Ed. Engl.*, 2014, **53**, 3720–3721.
20 C. Sikorska, S. Freza and P. Skurski, *J. Phys. Chem. A*, 2010, **114**, 2235–2239.
21 M. Czapla and P. Skurski, *Chem. Phys. Lett.*, 2015, **630**, 1–5.
22 M. Czapla and P. Skurski, *Phys. Chem. Chem. Phys.*, 2015, **17**, 19194–19201.
23 S. Senger and L. Radom, *J. Phys. Chem. A*, 2000, **104**, 7375–7385.
24 G. Zhong, B. Chan and L. Radom, *Org. Lett.*, 2009, **11**, 749–751.
25 M. Czapla and P. Skurski, *J. Phys. Chem. A*, 2015, **119**, 12868–12875.
26 G. L. Gutsev and A. I. Boldyrev, *Chem. Phys.*, 1981, **56**, 277–283.
27 X.-B. Wang, C.-F. Ding, L.-S. Wang, A. I. Boldyrev and J. Simons, *J. Chem. Phys.*, 1999, **110**, 4763–4771.
28 M. Czapla, I. Anusiewicz and P. Skurski, *Chem. Phys.*, 2016, **465–466**, 46–51.
29 F. A. Hohorst, L. Stein and E. Gebert, *Inorg. Chem.*, 1975, **14**, 2233–2236.
30 T. Drews, W. Koch and K. Seppelt, *J. Am. Chem. Soc.*, 1999, **121**, 4379–4384.
31 K. O. Christe, C. J. Schack and R. D. Wilson, *Inorg. Chem.*, 1977, **16**, 849–854.
32 J. E. Roberts and A. W. Laubengayer, *J. Am. Chem. Soc.*, 1957, **79**, 5895–5897.
33 K. O. Christe, D. A. Dixon, D. J. Grant, R. Haiges, F. S. Tham, A. Vij, V. Vij, T.-H. Wang and W. W. Wilson, *Inorg. Chem.*, 2010, **49**, 6823–6833.
34 M. D. Lind and K. O. Christe, *Inorg. Chem.*, 1972, **11**, 608–612.
35 J. F. Lehmann, G. J. Schrobilgen, K. O. Christe, A. Kornath and R. J. Suontamo, *Inorg. Chem.*, 2004, **43**, 6905–6921.
36 D. E. McKee, C. J. Adams and N. Bartlett, *Inorg. Chem.*, 1973, **12**, 1722–1725.
37 Z. Mazej and E. Goreshnik, *Inorg. Chem.*, 2008, **47**, 4209–4214.
38 H. S. A. Elliott, J. F. Lehmann, H. P. A. Mercier, H. D. B. Jenkins and G. J. Schrobilgen, *Inorg. Chem.*, 2010, **49**, 8504–8523.
39 J. F. Lehmann, D. A. Dixon and G. J. Schrobilgen, *Inorg. Chem.*, 2001, **40**, 3002–3017.
40 J. Bacon, P. A. W. Dean and R. J. Gillespie, *Can. J. Chem.*, 1970, **48**, 3413–3424.
41 W. W. Wilson, R. C. Thompson and F. Aubke, *Inorg. Chem.*, 1980, **19**, 1489–1493.
42 R. Faggiani, D. K. Kennepohl, C. J. L. Lock and G. J. Schrobilgen, *Inorg. Chem.*, 1986, **25**, 563–571.
43 R. J. Gillespie and K. C. Moss, *J. Chem. Soc. A*, 1966, 1170–1175.
44 B. Bonnet and G. Mascherpa, *Inorg. Chem.*, 1980, **19**, 785–788.
45 J. C. Culmann, M. Fauconet, R. Jost and J. Sommer, *New J. Chem.*, 1999, **23**, 863–867.
46 C. Lee, W. Yang and R. G. Parr, *Phys. Rev. B: Condens. Matter Mater. Phys.*, 1988, **37**, 785–789.
47 A. D. Becke, *Phys. Rev. A*, 1988, **38**, 3098–3100.
48 A. D. McLean and G. S. Chandler, *J. Chem. Phys.*, 1980, **72**, 5639–5648.
49 R. Krishnan, J. S. Binkley, R. Seeger and J. A. Pople, *J. Chem. Phys.*, 1980, **72**, 650–654.
50 J. A. Pople, M. Head-Gordon and K. Raghavachari, *J. Chem. Phys.*, 1987, **87**, 5968–5975.
51 J. Gauss and D. Cremer, *Chem. Phys. Lett.*, 1988, **150**, 280–286.
52 E. A. Salter, G. W. Trucks and R. J. Bartlett, *J. Chem. Phys.*, 1989, **90**, 1752–1766.
53 B. H. Besler, K. M. Merz Jr and P. A. Kollman, *J. Comput. Chem.*, 1990, **11**, 431–439.
54 M. J. Frisch, G. W. Trucks, H. B. Schlegel, G. E. Scuseria, M. A. Robb, J. R. Cheeseman, G. Scalmani, V. Barone, B. Mennucci, G. A. Petersson, H. Nakatsuji, M. Caricato, X. Li, H. P. Hratchian, A. F. Izmaylov, J. Bloino, G. Zheng, J. L. Sonnenberg, M. Hada, M. Ehara, K. Toyota, R. Fukuda, J. Hasegawa, M. Ishida, T. Nakajima, Y. Honda, O. Kitao, H. Nakai, T. Vreven, J. A. Montgomery Jr, J. E. Peralta, F. Ogliaro, M. Bearpark, J. J. Heyd,

E. Brothers, K. N. Kudin, V. N. Staroverov, R. Kobayashi, J. Normand, K. Raghavachari, A. Rendell, J. C. Burant, S. S. Iyengar, J. Tomasi, M. Cossi, N. Rega, J. M. Millam, M. Klene, J. E. Knox, J. B. Cross, V. Bakken, C. Adamo, J. Jaramillo, R. Gomperts, R. E. Stratmann, O. Yazyev, A. J. Austin, R. Cammi, C. Pomelli, J. W. Ochterski, R. L. Martin, K. Morokuma, V. G. Zakrzewski, G. A. Voth, P. Salvador, J. J. Dannenberg, S. Dapprich, A. D. Daniels, Ö. Farkas, J. B. Foresman, J. V. Ortiz, J. Cioslowski and D. J. Fox, *Gaussian 09, Revision A.02*, Gaussian, Inc, Wallingford CT, 2009.